tvst

Artificial Intelligence

An Intelligent Grading Model for Myopic Maculopathy Based on Long-Tailed Learning

Bo Zheng[1,2], Chen Wang[1], Maotao Zhang[1], Shaojun Zhu[1,2], Maonian Wu[1,2], Tao Wu[3], Weihua Yang[4], and Lu Chen[4]

[1] School of Information Engineering, Huzhou University, Huzhou, China
[2] School of Information Engineering, Zhejiang Province Key Laboratory of Smart Management & Application of Modern Agricultural Resources, Huzhou University, Huzhou, China
[3] School of Information Engineering, Zhejiang University of Technology, Hangzhou, China
[4] Shenzhen Eye Hospital, Shenzhen Eye Medical Center, Southern Medical University, Shenzhen, China

Correspondence: Weihua Yang, Shenzhen Eye Hospital, Shenzhen Eye Medical Center, Southern Medical University, Xinhu street 1333, Guangdong, Shenzhen 518000, China. e-mail: benben0606@139.com
Lu Chen, Shenzhen Eye Hospital, Shenzhen Eye Medical Center, Southern Medical University, Xinhu street 1333, Guangdong, Shenzhen 518000, China. e-mail: chenlu@sz-eyes.com

Received: October 19, 2024
Accepted: January 15, 2025
Published: March 6, 2025

Keywords: long-tail learning; myopic maculopathy; deep learning; diagnosis; grading

Citation: Zheng B, Wang C, Zhang M, Zhu S, Wu M, Wu T, Yang W, Chen L. An intelligent grading model for myopic maculopathy based on long-tailed learning. Transl Vis Sci Technol. 2025;14(3):4, https://doi.org/10.1167/tvst.14.3.4

Purpose: To develop an intelligent grading model for myopic maculopathy based on a long-tail learning framework, using the improved loss function LTBSoftmax. The model addresses the long-tail distribution problem in myopic maculopathy data to provide preliminary grading, aiming to improve grading capability and efficiency.

Methods: This study includes a data set of 7529 color fundus photographs. Experienced ophthalmologists meticulously annotated the ground truth. A new intelligent grading model for myopic maculopathy was constructed using the improved loss function LTBSoftmax, which predicts lesions by locally enhancing feature extraction with ND Block. Standard grading metrics were selected to evaluate the LTBSoftmax model.

Results: The improved model demonstrated excellent performance in diagnosing four types of myopic maculopathy, achieving a κ coefficient of 88.89%. Furthermore, the model's size is 18.7 MB, which is relatively smaller compared to traditional models, indicating that the model not only achieves a high level of agreement with expert diagnoses but is also more efficient in terms of both storage and computational resources. These metrics further validate the model's well-conceived design and superiority in practical applications.

Conclusions: The intelligent grading system, using long-tailed learning strategies, effectively improves the classification of myopic maculopathy, offering a practical grading tool for clinicians, particularly in areas with limited resources.

Translational Relevance: This model translates long-tail learning research into a practical grading tool for myopic maculopathy. It addresses data imbalance with the improved LTBSoftmax loss function, achieving high accuracy and efficiency. By enhancing feature extraction with ND Block, it provides reliable grading support for clinicians, especially in resource-limited settings.

Introduction

According to statistics, there are currently approximately 163 million individuals worldwide with myopic macular degeneration (MMD), with a prevalence rate of 2.7%. Among high myopia individuals, the prevalence of MMD is significantly higher, estimated at 20% to 30%, and this rate will likely rise as the global prevalence of high myopia continues to increase.[1] A 5-year follow-up study from the Gutenberg Health Study in Germany reported a myopic maculopathy prevalence of approximately 0.3% among 15,010 participants aged 35 to 74 years. Patients had more than a 50% chance of disease progression, with 20% developing new lesions.[2] Deng et al.[3] studied the population of children with high myopia in China. The results showed that myopic maculopathy had a signifi-

cant incidence among these children. The study found that approximately 10.3% of children with high myopia developed myopic maculopathy, and the incidence increased significantly with higher levels of myopia.

Myopic maculopathy refers to a series of degenerative changes in the macular area caused by high myopia, including chorioretinal atrophy, lacquer cracks, choroidal neovascularization, and macular atrophy.[4,5] These changes can lead to significant and often irreversible vision loss, making it one of the most severe complications of high myopia. Pathologic myopia is typically defined as a refractive error of ≤–6.00 diopters (D) or an axial length of ≥26.5 mm, accompanied by degenerative changes in ocular structures. Pathologic myopia can result in severe complications, such as myopic maculopathy, posterior staphyloma, and retinal detachment, making it one of the leading causes of visual impairment. Myopic maculopathy is the most severe, irreversible complication of high myopia and a major cause of vision loss and blindness.[6] Maculopathy diagnosis typically involves binocular ophthalmoscopy, color fundus photography, and optical coherence tomography (OCT). While effective, these methods require substantial resources. This limits access and delays timely treatment in resource-limited settings.[7] With the increase in myopia and high myopia populations, the number of patients with myopic maculopathy and research on medical aid grading of myopic maculopathy have increased.[8]

In recent years, deep neural networks with advanced data learning capabilities have seen growing application in the medical field.[9,10] Deep neural networks are primarily used in color fundus photographs, OCT, optical coherence tomography angiography (OCTA), fundus fluorescein angiography (FFA), and other bio-optical imaging in optical bioimaging for retinal diseases.[11–15] Compared to the limited research on myopic macular lesions, current deep learning–based studies on macular lesions have primarily focused on the identification of age-related macular lesions.[16–19] Fang et al.[20] developed an artificial intelligence (AI)–based pathologic myopia detection system for ophthalmology residency training, achieving a diagnostic accuracy of 88.6% using deep learning algorithms. Li et al.[21] reviewed advancements in imaging technologies for pathologic myopia and highlighted the role of AI, particularly in multimodal imaging, where AI achieved an accuracy of 92.1%, supporting early disease identification and clinical diagnosis. Meng et al.[22] proposed an AI classification method combining visual function and fundus features to identify high myopia, achieving 89.7% accuracy on multicenter data sets and improving clinical classification precision. Tan et al.[23] applied deep learning algorithms to fundus photographs for myopia diagnosis and integrated blockchain technology to advance AI-driven medical research. Their algorithm achieved an area under the curve (AUC) of 91% across multiple data sets, demonstrating excellent performance and cross-platform adaptability. El-Den et al.[24] reviewed the application of AI in detecting age-related macular degeneration (AMD), with some AI models achieving a diagnostic accuracy of 91.2%. Aranha et al.[25] proposed a deep transfer learning method that achieved an identification accuracy of 88.5% when processing low-quality fundus images. Du et al.[26] introduced a probabilistic contrastive learning approach to address data imbalance, improving model accuracy to 87.9%. Vaghefi et al.[27] achieved a diagnostic accuracy of 89.3% for intermediate dry AMD through multimodal retinal image analysis.

Building on the aforementioned research, many studies in the field utilize deep learning techniques, which depend on large, well-balanced data sets for effective training. However, medical imaging data often exhibit a long-tailed distribution, where mild cases significantly outnumber severe ones, leading to an imbalance in the data set.[28,29] Training models on such imbalanced data sets often results in suboptimal results, highlighting the need to address the challenges posed by long-tailed distributions in medical image classification. In response to these challenges, long-tailed learning has gained significant attention in both academia and industry in recent years.[30,31] The primary aim of long-tailed learning is to enhance model performance on imbalanced data sets by enhancing the recognition of minority classes. By using specialized training strategies or loss functions, long-tailed learning helps models better adapt to the distribution of minority samples, ultimately enhancing overall classification performance.[32,33] Chen et al.[34] used deep learning and an optimized long-tail learning method to segment the choroid in myopic fundus images, achieving 92.4% accuracy and addressing long-tail data challenges. Wang et al.[35] applied knowledge distillation to improve minority class lesion segmentation in diabetic retinopathy, reaching 91.7% accuracy and outperforming traditional methods. Yu and Zhu[36] developed a cross-modal network using multimodal imaging data to address long-tail issues in ophthalmic diseases, achieving an AUC of 0.94 and improving diagnostic accuracy by 8%.

These related studies highlight the significant potential of long-tailed learning methods in diagnosing and processing images related to macular diseases. However, specific challenges associated with the long-tailed distribution of myopic maculopathy data remain primarily unaddressed in existing research. To tackle

this issue, this study integrates long-tailed learning theory by employing an improved loss function to optimize the intelligent grading system for myopic maculopathy. The goal is to achieve preliminary grading diagnosis while enhancing both grading accuracy and efficiency.

Methods

Data Set

The color fundus images of myopic maculopathy analyzed in this study were obtained from partnering hospitals. Data collection used various models of nonmydriatic fundus cameras, including brands such as Topcon (Itabashi-ku, Tokyo, Japan), Canon (Ota-ku, Tokyo, Japan), and Zeiss (Oberkochen, Germany). To ensure consistent image quality and data reliability, the color fundus photography equipment at the partnering hospitals underwent regular quality checks and maintenance. The image collection was rigorously standardized, with controlled parameters including viewing angle, focal length, lighting intensity, and resolution. This standardization ensured a high degree of consistency and repeatability in image quality. All images were captured without pupil dilation to avoid potential retinal effects from mydriatic agents, better reflecting the true condition of the patients' fundus.

The study was conducted in accordance with the tenets of the Declaration of Helsinki and was based on a retrospective analysis of existing data. Informed verbal consent was obtained from all participants at the time of data collection for the use of their data in research.

The study utilized 7529 images with resolutions ranging from 2580 × 1920 to 2580 × 1920 pixels. All images were anonymized during postprocessing, and identifying information was removed to ensure data security and protect participant privacy. This provided a solid foundation for model development and analysis.

Table 1. Classification Results of LTBSoftmax Model

Characteristic	Training Set	Validation Set	Test Set
C0: Normal	540	136	161
C1: TF	2146	537	671
C2: DCA	917	230	287
C3: PCA	844	211	264
C4: MA	374	94	117
Total	4821	1208	1500

The partnering hospitals also provided ground-truth grading results, which were regarded as definite expert grading. These diagnoses were determined through a double-blind process by two ophthalmologists (L.C.). In cases where their diagnoses agreed, the result was accepted as the conclusive diagnosis. If a disagreement occurred, a senior ophthalmology (W.Y.) expert rendered the conclusive decision. The provided color fundus photographs included either normal cases or one of four types of myopic maculopathy, with each image receiving an individual grading. This study's grading criteria for myopic maculopathy were based on a grading scale for myopic maculopathy that the Meta-analysis for Pathologic Myopia Study Group in 2015 proposed.[37] The grading comprises the following: category 0, no macular lesions (normal); category 1, tesselated fundus (TF); category 2, diffuse chorioretinal atrophy (DCA); category 3, patchy chorioretinal atrophy (PCA); and category 4, macular atrophy (MA). Lacquer cracks, choroidal neovascularization, and Fuchs' spots were considered additional lesions and were excluded in this grading study, as shown in Figure 1.[4]

The training data for this study comprised 6029 color fundus photographs, including 676 normal color fundus photographs, 2683 tessellated color fundus photographs, 1147 diffuse chorioretinal atrophy images, 1055 patchy chorioretinal atrophy images, and 468 macular atrophy images. The test data set comprised 1500 color fundus photographs. The data set distribution is shown in Table 1.

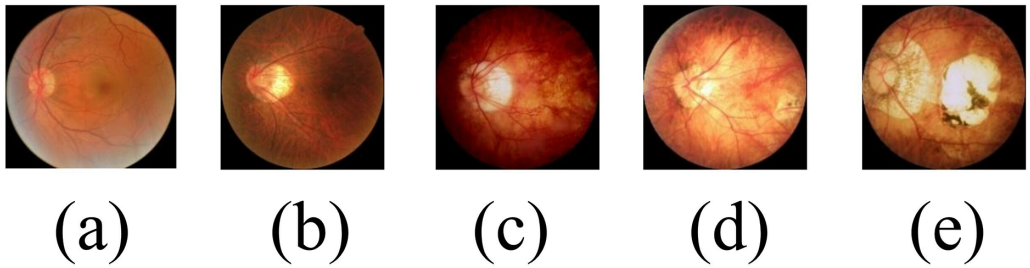

Figure 1. Color fundus photographs of different myopic maculopathy levels: (**a**) C0: normal; (**b**) C1: TF; (**c**) C2: DCA; (**d**) C3: PCA; (**e**) C4: MA.

Development of the LTBSoftmax Models

Algorithms

This study introduces an ND Block (Nonlocal Dependency) and an LTBSoftmax (Long-Tail Balanced Softmax) loss function to enhance lesion feature recognition in complex color fundus photographs. As depicted in Figure 2, these parts enable the model to capture both local details and global dependencies simultaneously, thereby improving grading accuracy.

The ND Block enhances the model's capacity to capture global features by computing the similarity features. First, the functions T(X) and P(X) apply linear transformations to the feature ***X***. The product of these transformations captures feature similarity, followed by normalization, using the Softmax function. Next, the normalized similarity matrix multiplies a third transformation G(X) extracting globally enhanced features. Finally, the model applies a weighted transformation and merges the result with

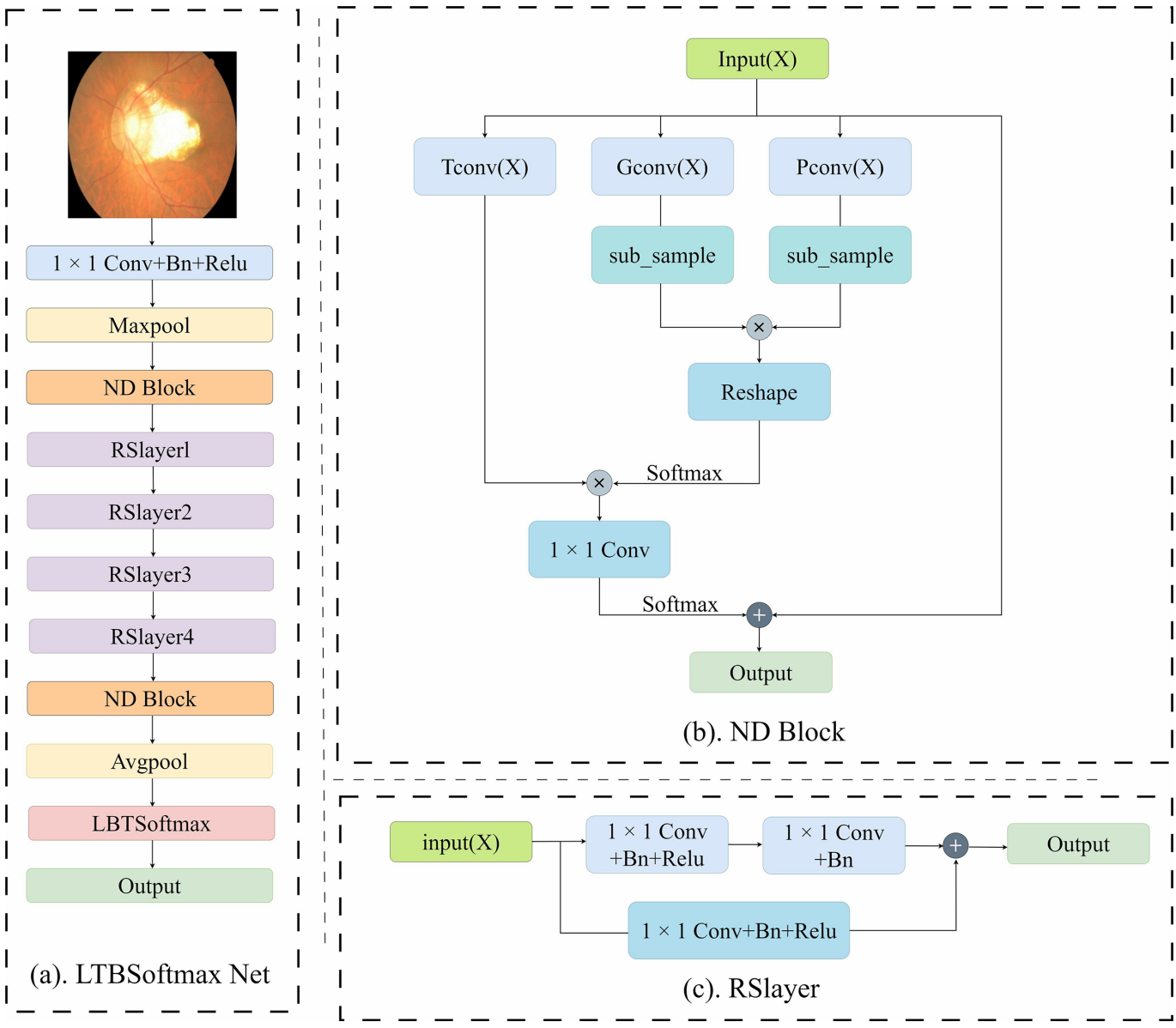

Figure 2. LTBSoftmax model architecture. (**a**) LTBSoftmax basic architecture: this model is designed for classification tasks. (**b**) ND Block, focused on global features: it captures global features, allowing information to be exchanged across different positions. (**c**) Residual layer, focused on specific features: it helps deep networks retain crucial information, enhancing training efficiency and mitigating the vanishing gradient problem.

the input $\boldsymbol{X}$ through residual connections, producing the final output.

Overall, the ND Block generates a weight matrix using the inner product and Softmax to weigh global features and merges these features with the original ones by residual connections, ensuring information integrity during feature fusion. The formula is as follows:

$$Z = X + W \cdot (\text{Softmax}(T(X) \cdot P(X)^T) \cdot G(X))$$

In designing the residual module, this study aims to enhance the model's representation ability and improve training stability through a series of computational steps. Specifically, the input feature $\boldsymbol{X}$ undergoes two consecutive linear transformation functions for initial feature extraction. After each linear transformation, the nonlinear activation functions are applied to the outputs, thereby enhancing the model's capability to capture complex features and extract higher-level representations.

After feature extraction and activation, this study employs a residual connection strategy by adding the original input $\boldsymbol{X}$ to the final deep feature representation to produce the output Y. In this way, the network can progressively extract higher-level features while maintaining information integrity, significantly improving the model's performance.

The Balanced-Meta Softmax (BALMS) loss function was proposed by the Innova team at NeurIPS 2020 to optimize classification objectives. Balanced Softmax was introduced to address the problem of overbalancing. The formula for the BALMS loss function is as follows:

$$\phi_j = \frac{n_j e^{n_j}}{\sum_{i=1}^{k} n_i e^{n_i}}$$

where n_j represents the total number of labels, and n_i represents the number of labels for each class.

Compared with the Balanced Softmax function, the key improvement introduced in this study is the combination of the advantages of long-tailed learning and metric learning. By introducing label distribution shifts and reducing intraclass distance while increasing interclass distance, this method mitigates the impact of the long-tail distribution on myopic maculopathy color fundus photographs. The specific implementation of the LTBSoftmax loss function is as follows:

$$Loss = \frac{1}{N} \sum_i -log \frac{n_j e^{s*\left(\cos\theta_{y_j} - m\right)}}{n_j e^{s*\left(\cos\theta_{y_j} - m\right)} + \sum_{i, i \neq j}^{N} n_i e^{s*\cos\theta_i}}$$

where $\cos\theta_{y_j}$ is used to compute x_j in the region of class y_j. The expression $\cos\theta_{y_j} - m$ requires that there be at least an m interval between class regions. The value of m depends on whether the data distribution has clear boundaries. If the boundary is clear, a larger m value can be set; if the boundary is unclear, a smaller m is required. This study focuses on grading myopic maculopathy, where the data distribution boundaries are not distinct, so a smaller m is set.

The formula $s * (\cos\theta_{y_j} - m)$ amplifies the cosine value by S-fold, as the cosine value is too small to effectively distinguish the variance. By amplifying the value by S-fold, the variance becomes more distinct, creating a significant "Matthew effect," thus optimizing convergence results.

Overall, the intelligent grading model for myopic maculopathy achieves a seamless integration of global and local features through the combination of an ND Block and a residual network module, with the optimized LTBSoftmax loss function. In diagnosing myopic maculopathy, the model precisely extracts fine features in the macular region using the residual network while capturing global dependencies through nonlocal attention. This characteristic endows the model with higher grading accuracy and stronger generalization ability when handling complex color fundus photographs, effectively supporting the early detection and recognition of subtle changes in the progression of maculopathy, thereby improving the reliability and efficiency of clinical grading.

Construction of Training and Testing Episodes

In this study, the training data consisted of 6029 color fundus photographs, with 4821 in the training set, 1208 in the validation set, and 1500 in the test set. To reduce computational complexity without compromising the visibility of retinal details, each color fundus photograph and its corresponding label map in the data set were resized to a resolution of 224 × 224 pixels. To reduce overfitting and improve the model's generalization ability, we applied data augmentation techniques to the original data set, including horizontal flipping, rotation, and contrast enhancement. Throughout 500 experimental training iterations, the proposed model was evaluated every 50 iterations. The model's training hyperparameters were set as follows: Adam optimizer with an initial learning rate of 0.02, a batch size of 4, and a binary cross-entropy loss function. The training strategies for other comparison methods were consistent with those outlined in their original studies. The deep learning methods used in the experiments were implemented based on the PyTorch library. The hardware configuration comprised an Intel Xeon Gold

5118 CPU at 2.30 GHz and a single Tesla V100 GPU (NVIDIA, Santa Clara, CA, USA) with 32 GB of memory.

Statistical Analysis

To compare the proposed myopic maculopathy grading model's performance with other state-of-the-art deep learning methods, three key evaluation metrics were employed to evaluate the similarity between the predicted masks and the ground truth: sensitivity, specificity, and accuracy. The variables TP, FP, TN, and FN represent true positives, false positives, true negatives, and false negatives, respectively. In subsequent experiments, the metrics employed include mean sensitivity (mSensitivity), mean specificity (mSpecificity), and mean accuracy (mAccuracy), where the prefix "m" indicates the average across all categories.

SPSS 22.0 statistical software (SPSS, Inc., Chicago, IL, USA) was employed for the analysis of the experimental results. The evaluation metrics included sensitivity, specificity, and accuracy, with a receiver operating characteristic (ROC) curve plotted to assess the model's performance. Higher sensitivity indicates a lower rate of missed diagnoses, while higher specificity suggests a lower rate of false positives. The consistency between the expert grading group and the model's grading results was assessed via the κ test. A κ value between 61% and 80% indicates substantial agreement, and a value above 80% indicates almost perfect agreement.

The formulas for κ value, sensitivity, specificity, and accuracy are as follows:

$$Sensitivity = \frac{TP}{TP + FN} \tag{1}$$

$$Specificity = \frac{TN}{TN + FP} \tag{2}$$

$$Accuracy = \frac{TP + TN}{TP + TN + FP + FN} \tag{3}$$

Results

This study tested the myopic maculopathy grading model using 1500 clinically acquired color fundus photographs. The expert grading group classified the images as follows: 161 normal color fundus photographs, 671 TF color fundus photographs, 287 DCA images, 264 PCA images, and 117 MA images.

Table 2 and Figure 3 present the grading results of the model. The grading model developed in this study produced the following grading results: 161 normal color fundus photographs, 648 TF color fundus photographs, 250 DCA images, 220 PCA images, and 102 MA images.

All models used in this study, including VGG16, ResNet50, RegNet, EfficientNet-B0, EfficientNet-B7, Softmax, Meta+Softmax, and Meta+BalancedSoftmax, are neural network models. Compared with the expert grading group, the myopic maculopathy grading model based on LTBSoftmax achieved sensitivities of 100.00%, 100.00%, 87.11%, 83.33%, and 87.18% in diagnosing normal (C0), TF (C1), DCA (C2), PCA (C3), and MA (C4), respectively. The specificity for diagnosing the five grades of myopic maculopathy categories was above 96%. The AUC values for the categories were 100.00%, 100.00%, 98.20%, 97.40%, and 99.10%, respectively. The model's κ value was 88.89%, indicating high grading consistency, and its accuracy reached 92.07%. The model size is 18.7 MB, smaller than other neural network models. The evaluation metrics for all eight models are shown in Table 3.

Among the seven models, the long-tail learning models outperformed the others, with LTBSoftmax achieving the highest κ and accuracy, particularly excelling in diagnosing TF and MA.

Table 2. Classification Results of LTBSoftmax Model

	LTBSoftmax					
Clinical	C0: Normal	C1: TF	C2: DCA	C3: PCA	C4: MA	Total
C0: Normal	161	0	0	0	0	161
C1: TF	0	646	22	11	1	680
C2: DCA	0	24	242	13	2	281
C3: PCA	0	1	23	222	14	260
C4: MA	0	0	0	18	100	118
Total	189	569	206	138	83	1500

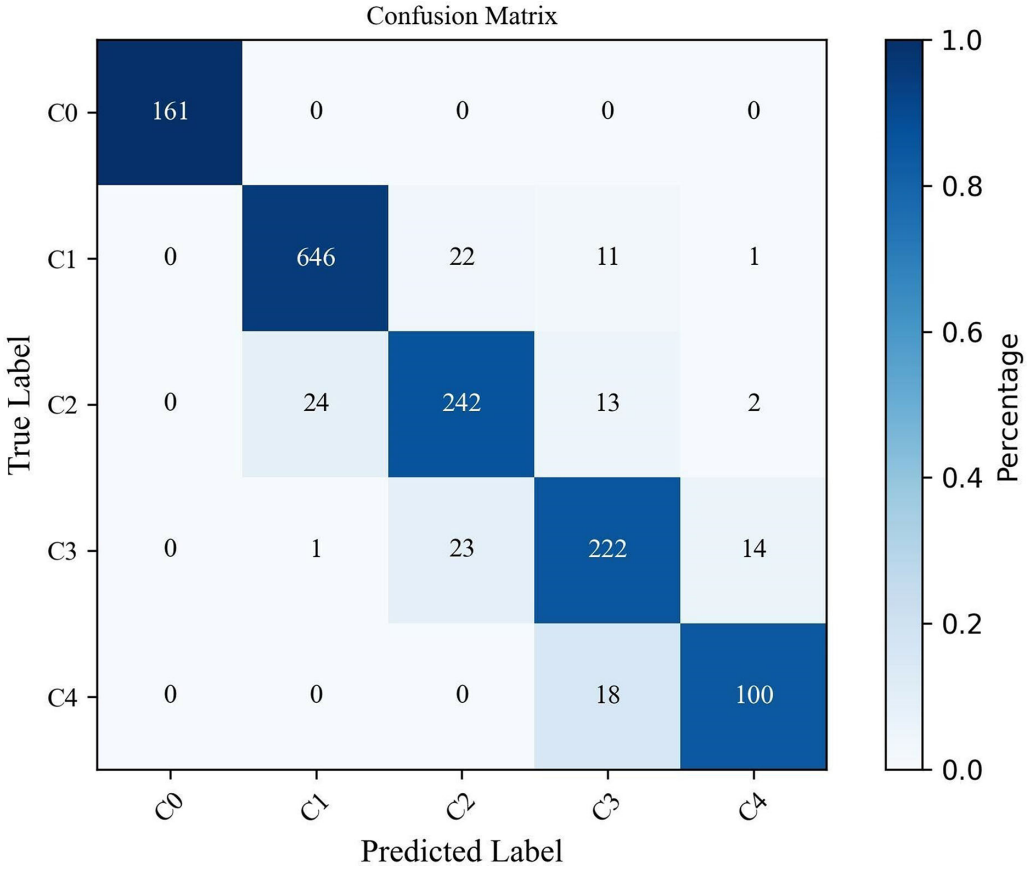

Figure 3. The confusion matrix shows the classification results for five clinical categories. The diagonal represents correct classifications, with color intensity indicating the number of samples.

Meta+BalancedSoftmax was better diagnosed with DCA, while EfficientNet-B0 was more effective in diagnosing TF. Except for the VGG16 model, all other models achieved 100% accuracy in diagnosing normal color fundus photographs. Figure 4 presents the ROC curves comparing the grading of normal color fundus photographs and four types of myopic maculopathy across the eight models. Figure 5 shows the heatmap generated during the recognition process by the model.

Discussion

Holden et al.[1] observed a progressive increase in the prevalence of myopic maculopathy. Recently, the number of near-sighted people has been gradually increasing worldwide, meaning the likelihood of myopic maculopathy is also increasing. Severe myopic maculopathy can cause loss of central vision. As people pay more attention to eye health, screening for myopic maculopathy using color fundus photographs can help patients understand the severity and progression of the disease and provide targeted treatment as early as possible, which can reduce or delay vision loss caused by myopic maculopathy. Chinese primary care and nonmedical institutions, such as optometry and dispensing centers, see many people with myopia but lack the professional grading techniques and are often unable to make graded diagnoses of different levels of myopic maculopathy. Therefore, developing a grading model for myopic maculopathy that can be used in routine computers can help doctors in the initial screening of myopic maculopathy, expand the application scenarios of myopic maculopathy grading, and improve the efficiency of grading.

Compared with the traditional deep learning model, this study's model uses LTBSoftmax instead of Softmax. Additionally, compared with traditional Softmax, LTBSoftmax considers the influence of the label distribution on the model training and refers to the metric learning method, which narrows each class to the target domain by narrowing the intraclass distance and increasing the class spacing, and widens the spacing between classes to improve the model's classification ability. This study uses MetaSampler for

Table 3. Evaluating the Grading Accuracy of the LTBSoftmax Model on a Long-Tailed Myopic Maculopathy Data Set

Model	Sensitivity, %	Specificity, %	F1-Score, %	AUC, %	95% CI	κ, %	Accuracy, %	Size (MB)
VGG16								
C0: normal	99.38%	99.18%	96.39%	99.60%	0.994–0.999	68.12%	77.53%	512
C1: TF	91.36%	88.54%	88.91%	91.60%	0.900–0.932			
C2: DCA	61.32%	92.75%	63.88%	82.40%	0.793–0.855			
C3: PCA	66.29%	89.81%	61.95%	83.00%	0.799–0.860			
C4: MA	33.33%	98.77%	45.09%	75.80%	0.701–0.816			
Resnet50								
C0: normal	100.00%	100.00%	100.00%	100.00%	1.000–1.000	79.39%	85.27%	90
C1: TF	94.93%	94.81%	94.30%	98.60%	0.981–0.991			
C2: DCA	80.49%	93.82%	77.91%	95.60%	0.945–0.967			
C3: PCA	61.36%	96.52%	69.08%	93.50%	0.921–0.949			
C4: MA	75.21%	95.66%	66.42%	95.00%	0.932–0.967			
RegNet								
C0: normal	100.00%	100.00%	100.00%	100.00%	1.000–1.000	87.12%	90.80%	15.1
C1: TF	95.98%	96.54%	95.98%	99.40%	0.992–0.997			
C2: DCA	90.24%	94.81%	85.06%	98.20%	0.976–0.987			
C3: PCA	76.52%	97.57%	81.45%	97.30%	0.964–0.982			
C4: MA	82.05%	98.70%	83.12%	99.00%	0.985–0.995			
EfficientNet-B0								
C0: normal	100.00%	100.00%	100.00%	100.00%	1.000–1.000	87.76%	91.27%	15.6
C1: TF	96.57%	96.62%	96.21%	99.40%	0.992–0.997			
C2: DCA	88.50%	95.38%	85.09%	98.20%	0.977–0.988			
C3: PCA	80.30%	97.33%	83.30%	97.40%	0.966–0.983			
C4: MA	83.76%	98.48%	85.00%	98.50%	0.978–0.993			
EfficientNet-B7								
C0: normal	100.00%	99.78%	99.08%	100.00%	1.000–1.000	87.39%	91.00%	245
C1: TF	97.17%	95.78%	96.02%	99.40%	0.991–0.997			
C2: DCA	82.93%	97.11%	85.00%	98.10%	0.975–0.987			
C3: PCA	77.65%	97.98%	83.00%	96.80%	0.958–0.978			
C4: MA	93.16%	97.32%	82.89%	99.00%	0.985–0.995			
Meta+Softmax								
C0: normal	100.00%	100.00%	100.00%	100.00%	1.000–1.000	85.78%	89.87%	18.7
C1: TF	96.27%	96.38%	95.92%	99.30%	0.990–0.996			
C2: DCA	81.53%	97.03%	84.02%	97.10%	0.970–0.983			
C3: PCA	84.47%	94.17%	79.79%	96.30%	0.955–0.977			
C4: MA	71.79%	98.99%	78.14%	98.30%	0.980–0.994			
Meta+BalancedSoftmax								
C0: normal	100.00%	100.00%	100.00%	100.00%	1.000–1.000	88.11%	91.53%	18.7
C1: TF	95.98%	96.50%	95.83%	99.40%	0.991–0.996			
C2: DCA	97.17%	96.02%	96.17%	99.50%	0.992–0.997			
C3: PCA	85.71%	96.78%	86.01%	98.30%	0.977–0.988			
C4: MA	81.82%	97.25%	84.05%	97.30%	0.965–0.982			
LTBSoftmax (ours)								
C0: normal	100.00%	99.93%	99.69%	100.00%	1.000–1.000	88.89%	92.07%	18.7
C1: TF	100.00%	99.93%	99.69%	100.00%	1.000–1.000			
C2: DCA	87.11%	96.78%	86.81%	98.20%	0.975–0.988			
C3: PCA	83.33%	97.57%	85.60%	97.40%	0.961–0.981			
C4: MA	87.18%	99.06%	85.96%	99.10%	0.986–0.996			

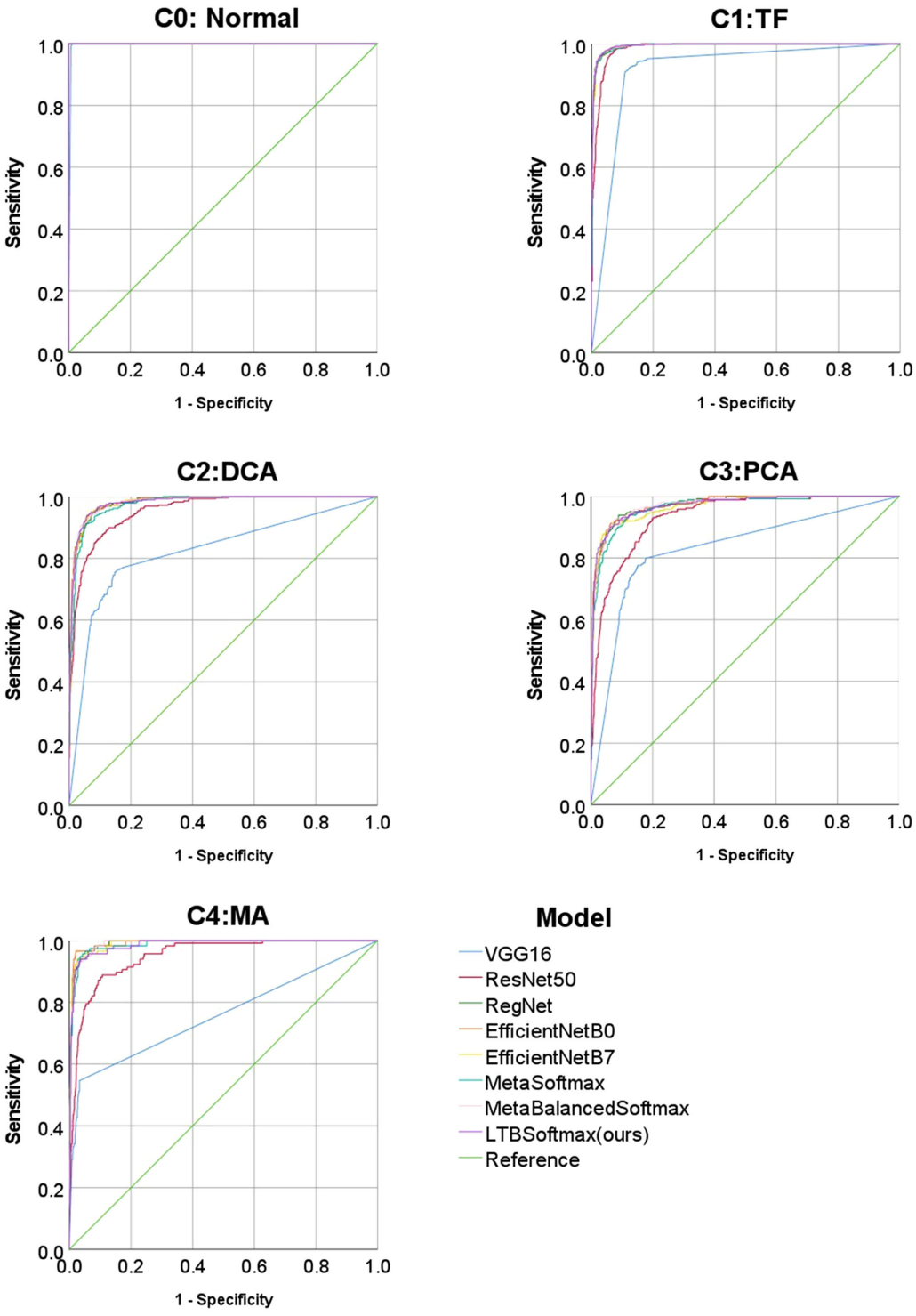

Figure 4. ROC of the seven models for normal, TF, DCA, PCA, and MA.

data sampling to dynamically learn the current optimal sampling rate, which is used to reduce the overweight problem that may be caused by the label distribution.

The partner hospital provided clinical training data for 7529 color fundus photographs, of which 6029 were used for training, with the highest and lowest number of training images being 2146 for TF and 374 for MA, respectively. The number of TF images was almost six times that of MA images, more than twice that of DCA images, and almost three times

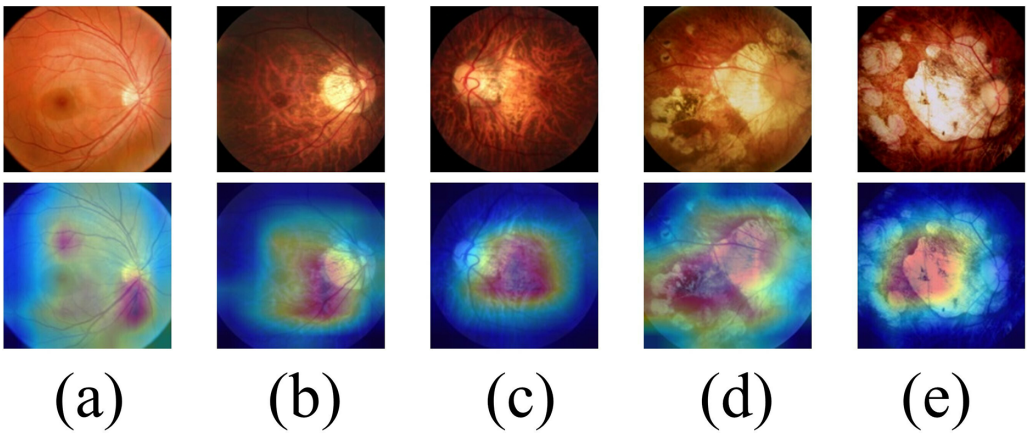

Figure 5. This figure shows the areas of focus for the LTBSoftmax model when identifying different stages of age-related macular degeneration.

that of PCA images. According to Table 3, the traditional neural network results are more likely to be biased toward the TF class and will cause poor performance in other classes. For example, for the traditional deep neural networks VGG16 and ResNet50, although their sensitivity to the TF class was 0.914 and 0.949, respectively, their sensitivity to the PCA class was 0.663 and 0.614, respectively, and their sensitivity to the MA class was 0.333 and 0.752, respectively. While this study used the LTBSoftmax model, despite its sensitivity and specificity for the TF class, the overall accuracy and κ value were the highest, and it performed well in a few classes, PCA and MA, and had the highest sensitivity of 0.833 in the PCA class and the highest specificity of 0.991 in MA. Conversely, EfficientNet-B7, although it had the highest sensitivity of 0.932 in the MA class, its sensitivity in PCA was almost the lowest at 0.777. These data suggest that in some classes, the long-tail distribution impacts EfficientNet-B7. Moreover, no studies on the influence of the long-tailed distribution on the construction of the myopic macular lesion model and on the classification and diagnosis of myopic macular lesions are currently available.

Shi et al.[17] used deep neural networks to screen color fundus photographs for the presence and severity of myopic macular lesions, defining C1 as a mild lesion and C2 and above as a severe lesion, with a sensitivity and specificity of 0.839 and 0.952, respectively, for diagnosing the severity of myopic macular lesions. The study only initially classified myopic macular lesions according to lesion severity and did not achieve C0 to C4. This study achieved a one-time five-classification grading and was no longer limited to binary screening of lesion severity.

The sensitivity and specificity of the other neural network models, such as DCA for diffuse atrophy (84.44% and 94.5%), PCA for patchy atrophy (87.22% and 96.02%), and MA for macular atrophy (87.22% and 96.02%), demonstrate solid performance. However, compared to the other neural network models, our proposed model significantly improves performance, particularly in underrepresented classes, with higher overall accuracy and the best sensitivity in PCA (0.833) and MA (0.991), highlighting its superior ability to handle imbalanced data.

In BALMS that the Innova's team proposed at NeurIPS 2020,[38] it is assumed that the labeling distribution affects the regular Softmax using Bayes' theorem, and the multinomial distribution exponential family form re-derives the Softmax to finally obtain a balanced Softmax suitable for the long-tailed problem. The balanced Softmax can approximately minimize the upper bound of the generalization error in long-tailed settings. Liu et al.[39] introduced SphereFace, which applies metric learning by adding a margin constraint on the angle to the modified Softmax loss, improving intraclass similarity while enhancing interclass differentiation. In 2018, Zhang et al.[40] further improved SphereFace by introducing additional parameters and scaling factors, reducing the probability of corresponding labeled terms and increasing the loss. Compared with these previous studies, this study combines long-tailed and metric learning approaches to improve the base Softmax by integrating both improvements. Combined with MetaSampler, which automatically learns the optimal sampling rate, this enhances the model's classification performance.

In practical applications, medical image data sets typically exhibit a long-tailed distribution. Traditional deep learning models trained on long-tailed

samples tend to be biased toward categories with larger sample sizes, resulting in poorer performance for categories with fewer samples. In this study, the myopic maculopathy data set exhibited a long-tailed distribution, as the sample size of patients with severe myopic maculopathy was significantly smaller than that of patients with mild disease. In future work, we aim to mitigate the impact of long-tailed distribution on the grading model by collecting more color fundus photographs of patients with severe disease to expand the data set.

In conclusion, this research presents a novel long-tailed learning approach for the intelligent grading of myopic maculopathy, effectively addressing the challenges posed by imbalanced data in medical image analysis. By integrating a nonlocal attention mechanism and the optimized LTBSoftmax loss function, the proposed model significantly improves grading performance, especially in underrepresented classes. These findings demonstrate the potential of long-tailed learning to enhance AI applications in ophthalmology, offering more accurate and efficient grading tools for myopic maculopathy. This approach could improve early detection and grading of myopic maculopathy, particularly in resource-limited settings, ultimately supporting better treatment outcomes for patients worldwide.

Acknowledgments

Supported by the National Natural Science Foundation of China (Grant No. 61906066), Sanming Project of Medicine in Shenzhen (No. SZSM202311012), and Postgraduate Research and Innovation Project of Huzhou University (No. 2022KYCX35).

Data Sets: The data were acquired from cooperative hospitals, which have not permitted researchers to share their data. Data requests can be made to study via this email: benben0606@139.com.

Disclosure: **B. Zheng**, None; **C. Wang**, None; **M. Zhang**, None; **S. Zhu**, None; **M. Wu**, None; **T. Wu**, None; **W. Yang**, None; **L. Chen**, None

References

1. Holden BA, Fricke TR, Wilson DA, et al. Global prevalence of myopia and high myopia and temporal trends from 2000 through 2050. *Ophthalmology*. 2016;123:1036–1042.
2. Wild P, Zeller T, Beutel M, et al. The Gutenberg health study. *Bundesgesundheitsblatt Gesundheitsforschung Gesundheitsschutz*. 2012;55:824–830.
3. Deng J, Xu X, Pan CW, et al. Myopic maculopathy among Chinese children with high myopia and its association with choroidal and retinal changes: the SCALE-HM study. *Br J Ophthalmol*. 2024;108(5):720–728.
4. Yokoi T, Ohno-Matsui K. Diagnosis and treatment of myopic maculopathy. *Asia Pac J Ophthalmol*. 2018;7:415–421.
5. Ohno-Matsui K, Wu P-C, Yamashiro K, et al. IMI pathologic myopia. *Invest Ophthalmol Vis Sci*. 2021;62:5.
6. Chen Y, Yang S, Liu R, et al. Forecasting myopic maculopathy risk over a decade: development and validation of an interpretable machine learning algorithm. *Invest Ophthalmol Vis Sci*. 2024;65:40.
7. Ng DS, Chan LK, Lai TY. Myopic macular diseases: a review. *Clin Exp Ophthalmol*. 2023;51:229–242.
8. Asensio-Sánchez VM. Myopic maculopathy in children and adolescents with high myopia. *JAMA Ophthalmol*. 2024;142(10):982–982.
9. Liu Y-H, Li L-Y, Liu S-J, et al. Artificial intelligence in the anterior segment of eye diseases. *Int J Ophthalmol*. 2024;17:1743.
10. Yang W-H, Shao Y, Xu Y-W. Guidelines on clinical research evaluation of artificial intelligence in ophthalmology (2023). *Int J Ophthalmol*. 2023;16:1361.
11. Zhu S, Zhan H, Yan Z, et al. Prediction of spherical equivalent refraction and axial length in children based on machine learning. *Indian J Ophthalmol*. 2023;71:2115–2131.
12. Yao J, Lim J, Lim GYS, et al. Novel artificial intelligence algorithms for diabetic retinopathy and diabetic macular edema. *Eye Vis*. 2024;11:23.
13. Ohno-Matsui K, Takahashi H, Mao Z, Nakao N. Determining posterior vitreous structure by analysis of images obtained by AI-based 3D segmentation and ultrawidefield optical coherence tomography. *Br J Ophthalmol*. 2023;107:732–737.
14. Li Z, Wang L, Wu X, et al. Artificial intelligence in ophthalmology: the path to the real-world clinic. *Cell Rep Med*. 2023;4(7):101095.
15. Zheng B, Zhang M, Zhu S, et al. Research on an artificial intelligence-based myopic maculopathy grading method using EfficientNet. *Indian J Ophthalmol*. 2024;72:S53–S59.
16. Guo Y, Peng Y. CARNet: Cascade attentive RefineNet for multi-lesion segmentation of diabetic retinopathy images. *Complex Intell Syst*. 2022;8:1681–1701.

17. Shi C, Liu L, Wang Y, Wang Z. Research on screening system of myopic maculopathy based on deep convolution neural network. *Chin J Exp Ophthalmol*. 2021;39(7):602–608.
18. Ricardi F, Oakley J, Russakoff D, et al. Validation of a deep learning model for automatic detection and quantification of five OCT critical retinal features associated with neovascular age-related macular degeneration. *Br J Ophthalmol*. 2024;108:1436–1442.
19. Domínguez C, Heras J, Mata E, Pascual V, Royo D, Zapata MÁ. Binary and multi-class automated detection of age-related macular degeneration using convolutional-and transformer-based architectures. *Comput Methods Programs Biomed*. 2023;229:107302.
20. Fang Z, Xu Z, He X, Han W. Artificial intelligence-based pathologic myopia identification system in the ophthalmology residency training program. *Front Cell Dev Biol*. 2022;10:1053079.
21. Li Y, Foo L-L, Wong CW, et al. Pathologic myopia: advances in imaging and the potential role of artificial intelligence. *Br J Ophthalmol*. 2023;107:600–606.
22. Meng J, Song Y, He W, et al. A novel artificial intelligence-based classification of highly myopic eyes based on visual function and fundus features. *Transl Vis Sci Technol*. 2024;13:12.
23. Tan T-E, Anees A, Chen C, et al. Retinal photograph-based deep learning algorithms for myopia and a blockchain platform to facilitate artificial intelligence medical research: a retrospective multicohort study. *Lancet Digital Health*. 2021;3:e317–e329.
24. El-Den NN, Elsharkawy M, Saleh I, et al. AI-based methods for detecting and classifying age-related macular degeneration: a comprehensive review. *Artif Intell Rev*. 2024;57:237.
25. Aranha GD, Fernandes RA, Morales PH. Deep transfer learning strategy to diagnose eye-related conditions and diseases: an approach based on low-quality fundus images. *IEEE Access*. 2023;11:37403–37411.
26. Du C, Wang Y, Song S, Huang G. Probabilistic contrastive learning for long-tailed visual recognition. *IEEE Trans Pattern Anal Machine Intell*. 2024;46(9):5890–5904.
27. Vaghefi E, Hill S, Kersten HM, Squirrell D. Multimodal retinal image analysis via deep learning for the diagnosis of intermediate dry age-related macular degeneration: a feasibility study. *J Ophthalmol*. 2020;2020:7493419.
28. Wu Z, Guo K, Luo E, et al. Medical long-tailed learning for imbalanced data: bibliometric analysis. *Comput Methods Programs Biomed*. 2024;247:108106.
29. Chen Z, Chen J, Feng Y, et al. Imbalance fault diagnosis under long-tailed distribution: challenges, solutions and prospects. *Knowledge Based Syst*. 2022;258:110008.
30. Zhang Y, Kang B, Hooi B, Yan S, Feng J. Deep long-tailed learning: a survey. *IEEE Trans Pattern Anal Machine Intell*. 2023;45:10795–10816.
31. Fang C, Cheng L, Mao Y, et al. Separating noisy samples from tail classes for long-tailed image classification with label noise. *IEEE Trans Neural Netw Learn Syst*. 2023;35(11):16036–16048.
32. Peifeng G, Xu Q, Wen P, Yang Z, Shao H, Huang Q. Feature directions matter: Long-tailed learning via rotated balanced representation. *Proceedings of the 40th International Conference on Machine Learning*. 2023;202:27542–27563.
33. Vu D-Q, Phung TT, Wang J-C, Mai ST. LCSL: long-tailed classification via self-labeling. *IEEE Trans Circuits Syst Video Technol*. 2024;34(11): 12048–12058.
34. Chen H-J, Huang Y-L, Tse S-L, et al. Application of artificial intelligence and deep learning for choroid segmentation in myopia. *Transl Vis Sci Technol*. 2022;11:38.
35. Wang Y, Hou Q, Cao P, Yang JR, Zaiane O. Lesion-aware knowledge distillation for diabetic retinopathy lesion segmentation. *Appl Intell*. 2024;54:1937–1956.
36. Yu Y, Zhu H. Transformer-based cross-modal multi-contrast network for ophthalmic diseases diagnosis. *Biocybernet Biomed Eng*. 2023;43:507–527.
37. Ohno-Matsui K, Kawasaki R, Jonas JB, et al. International photographic classification and grading system for myopic maculopathy. *Am J Ophthalmol*. 2015;159:877–883.e877.
38. Ren J, Yu C, Ma X, Zhao H, Yi S. Balanced meta-softmax for long-tailed visual recognition. *Adv Neural Inform Process Syst*. 2020;33:4175–4186.
39. Liu W, Wen Y, Yu Z, Li M, Raj B, Song L. Sphereface: deep hypersphere embedding for face recognition. In: *Proceedings of the IEEE Conference on Computer Vision and Pattern Recognition*. Piscataway, NJ: IEEE; 2017:212–220.
40. Zhang Y, Hooi B, Hong L, Feng J. Self-supervised aggregation of different experts for long-tail recognition of test marks. *Adv Neural Inf Process Syst*. 2022;35:34077–34090.